The electronic structure and stability of transition metal nanotips. I

1995 J. Phys.: Condens. Matter 7 6625

(http://iopscience.iop.org/0953-8984/7/33/004)

J. Phys.: Condens. Matter 7 (1995) 6625–6640. Printed in the UK

The electronic structure and stability of transition metal nanotips—part I

H Ness† and F Gautier‡

† Department of Physics, University of Durham, South Road, Durham DH1 3LE, UK
‡ IPCMS–GEMME, Bâtiment 69, 23 rue du Loess, 67037 Strasbourg, France

Received 18 May 1995

Abstract. A detailed theoretical study of the electronic structure of transition metal nanotips is performed in the tight-binding scheme. The real space recursion method is used to determine the local densities of states (LDOS) of the nanotips. We consider more especially the W supported pyramidal tips and W pyramidal clusters with different morphologies. The apex LDOS of perfect supported tips are found to be quite different from those of surfaces and of clusters having the same morphology. The stability of the supported nanotips of different morphologies is also examined.

1. Introduction

Since the pioneering work of Binnig *et al* [1,2], many experimental and theoretical studies have been devoted to the near-field microscopies (scanning tunnelling microscopy—STM—and atomic force microscopy—AFM) and more especially to the conditions to achieve atomic resolution. The atomic and electronic structures of nanotips and of surfaces and their modifications when the two systems interact are essential to understand the observed images. However up to now and even if the atomic resolution can be experimentally obtained by STM and AFM, there is no detailed theoretical knowledge of the role of these parameters on the contrast. The present paper is devoted to this problem and more especially to the electronic structure of *transition metal* nanotips in relation to their morphology, to the influence of the interaction of the nanotip with its support and finally to the general trends of the stability of such nanotips. The influence of the tip/sample interaction on the electronic structure of the considered system will be presented in the second part of this study [3].

In this introduction, we first summarize the present knowledge of the properties of nanotips (subsection 1.1). Then we discuss briefly the theoretical models for STM in relation to the importance of the tip electronic structure (subsection 1.2). Finally we present the summary of this paper (subsection 1.3).

1.1. Transition metal nanotips

Different experimental techniques have been proposed for the production of nanotips with a well controlled geometry [4–6]. For example, Vu Thien Binh *et al* have developed techniques based on ultrahigh-vacuum heat treatments in the presence of an electrical field [5]. Nanotips can be sharpened *in situ* in a reproducible manner. Using such techniques it

0953-8984/95/336625+16$19.50

is possible to obtain W protrusions ending in one atom [5, 6]. The analysis at the atomic scale of the structure of these W tips has been performed by field ion microscopy [5]. The successive field ion diagrams, obtained after a progressive field evaporation, show a monatomic apex, a three-atom second layer, a seven-atom third layer and so on. These tips were always found to be localized around the ⟨111⟩ axis of the W tip's support.

Such nanotips can be used as electron sources with high brightness for conventional microscopies. Because of their atomic dimensions, they produce coherent electron beams and have been used for holography experiments [7]. Finally they are of high interest for the near-field microscopies, the atomic structure of the topmost end of the tips playing an important role in such microscopies.

Up to now no detailed theoretical study of the electronic structure of such nanotips has been performed. However experimentally some peculiar features have been exhibited by field emission electron spectroscopy (FEES) on nanotips [8]. For example, the total energy distribution spectra obtained for monatomic apex tips are characterized by well separated peaks. These spectra cannot be fitted with the Fowler–Nordheim theory and have been interpreted by the presence of localized band structures at the tip apex through which resonant tunnelling occurs. These experiments show the need of a detailed understanding of the electronic structure of such nanotips in relation to their atomic structure.

1.2. Tip electronic structure and models for the tunnelling current

The most popular theory for the STM [9] is based on two important assumptions. (i) The tunnelling current between weakly coupled electrodes is calculated within the Bardeen perturbation scheme [10]. (ii) The tip is assumed to be spherical. Within this theory, the tunnelling current is found to be proportional to the product of the unperturbed surface local density of states (LDOS) $\rho(r_0, \varepsilon_F)$ at the Fermi energy ε_F and at the r_0 tip position multiplied by the density of states per unit volume $D_t(\varepsilon_F)$ of the probe tip. Therefore the STM images in the constant-current mode are viewed as constant surface LDOS. This theory allows us to understand the general features of the STM images. Nevertheless, it cannot explain some peculiar effects such as the observed high corrugation on Au and Al close-packed surfaces [11] so the two basic assumptions used in the above theory have to be re-examined. Let us now discuss briefly our present theoretical understanding of the influence of the tip's electronic structure on the STM images.

The roles of the atomic and electronic structure of nanotips on STM images were first pointed out by Ohnishi and Tsukuda [12]. The first-principles calculations of the electronic structure of pyramidal W clusters they performed show that a dangling bond state near ε_F exists on the apex atom of both W_4 and W_5 clusters, this state being quite well described by a d_{z^2} state. Furthermore they use the STM model of Tsukada and Shima [13], which also relies on the Bardeen approximation, in order to calculate the tunnelling current between the Si sample and the W cluster tips [12]. They find that the current is primarily generated by the d_{z^2} tip state considered above.

On the other hand, Chen has calculated explicitly the tunnelling matrix elements, used in the Bardeen approach, for different tip states [14]. These matrix elements are found to be proportional to the partial derivatives of the unperturbed sample wave functions taken at the position r_0 of the tip. Using his 'derivative rule' for model simple metals, Chen has found that the contribution of p_z and d_{z^2} tip orbitals yields an enhancement of the corrugation compared to s states [14]. This is assumed to be a possible explanation for the high corrugation observed on compact metal surfaces. Within his framework, Chen also obtains, as observed in some STM images, a contrast inversion when an $m \neq 0$ state

dominates the tip states near ε_F over $m = 0$ (p_z of d_{z^2}) state [15].

These two last models emphasize the importance of the electronic structure of nanotips for the understanding of STM images.

1.3. Summary

The purpose of this paper is to clarify the dependence of the tip electronic structure upon its morphology and to obtain the general trends of the energetic stability of such nanotips. The tips are assumed to be pyramids whose apexes are of atomic dimensions. Tips having the same shape as those obtained experimentally by Vu Thien Binh [5,6] are also considered. We restrict the present study to transition metal tips and more especially to W tips which are supported or not. The geometrical complexity of such systems involves supercells too large for *ab initio* calculations and hence computing times too large to determine the band structure of these systems. This is why we choose the tight-binding approach to describe the band structure of the considered systems. Furthermore, we use the simplicity of the real space recursion method in order to calculate the LDOS of such systems.

The content of this paper is as follows. In section 2 we present the model we use for the energy and the method of calculation for the electronic structure of the systems we consider. In section 3 we discuss the results we obtain for the electronic structure of supported and cluster tips. Section 4 is devoted to the study of the energy stability for different tip morphologies. Finally we summarize the most significant results we obtained (section 5).

2. Model for the energy and method of calculation

As previously mentioned, we use in this paper the tight-binding approximation and the real space recursion method, which does not rely on periodicity assumptions. Within this model, the total energy $E = E_{bs} + E_r$ results from two contributions: (i) the attractive band term E_{bs} which is obtained from the LDOS and (ii) the repulsive term E_r which is described by a pair potential and insures the crystal stability. This model is sufficient to obtain a realistic description of transition metal bulk and surface properties, phase stability and chemisorption [16,17]. Let us now describe the assumptions we use here for the calculations of the LDOS and for the tip morphology.

2.1. Band structure and repulsive energies

In this first study, we have restricted our attention only to 'd' bands, so that the energy E_{bs} is the one-electron contribution due to these 'd' electrons. The tight-binding Hamiltonian

$$H = \sum_{i,\lambda} |i\lambda\rangle \varepsilon_{i\lambda} \langle i\lambda| + \sum_{\substack{i,j\neq i \\ \lambda,\mu}} |i\lambda\rangle t_{\lambda\mu}(\boldsymbol{R}_{ij}) \langle j\mu|$$

is obtained from the energy levels $\varepsilon_{i\lambda}$ and the hopping integrals $t_{\lambda\mu}(\boldsymbol{R}_{ij})$ between two sites i and j (the vector $\boldsymbol{R}_{ij}$ joins these two atoms and R_{ij} is the corresponding distance); λ and μ label the 'd' orbitals ($xy, xz, yz, x^2 - y^2, 3z^2 - r^2$). The hopping integrals are described by a linear combination of the three Slater–Koster parameters ddσ, ddπ, ddδ [18]. These parameters are assumed to vary exponentially with the interatomic distance:

$$\mathrm{dd}\chi(R_{ij}) = \mathrm{dd}\chi_1 \exp(-q(R_{ij} - R_1)/(R_1) \qquad \chi = \sigma, \pi, \delta \qquad q = 3$$

R_n being the equilibrium distance between two nth-nearest neighbours. For example, the values of the $dd\chi_1$ parameters between first-nearest neighbours for W are fitted to the LDA band structure of W [19] and are chosen as those used by Treglia *et al* ($dd\sigma_1 = -1.4456$ eV, $dd\pi_1 = 0.7984$ eV, $dd\delta_1 = 0$) [20].

For the study of the electronic structure of the tips and surfaces, we assumed that the $t(\boldsymbol{R})$ are non-zero only between first- and second-nearest neighbours. We have also tried other analytical forms for the hopping integrals to test the sensitivity of the results to such an assumption. This will be necessary for the determination of the tip/sample interaction forces which requires an analytical continuation of the hopping integrals $t(\boldsymbol{R})$ to avoid artificial discontinuities in the numerical calculation. For example, we have performed calculations with continuously decaying $t(\boldsymbol{R})$ having a hyperbolic cosine form and zero values when $R \geqslant R_4$. As will be shown later, the results we obtain for such a distance dependence do not significantly modify the LDOS either for the atoms of the surfaces or for those of the tips.

In our calculations, we required self-consistent local neutrality on each atomic site. This approximation is valid for alloys, compounds and clusters when the electronegativity difference between the constituents is not too large, which is our case. The self-consistent procedure is performed assuming that the local energy levels $\varepsilon_{i\lambda}$ are independent of the considered 'd' orbital ($\varepsilon_{i\lambda} = \varepsilon_i$), i.e. neglecting the crystalline field effects. These levels are determined to obtain the band filling within the local neutrality with an accuracy of 10^{-4}. In practice, this self-consistent procedure is performed for the tip atoms and for the three first planes of the tip's support (TSp) from its surface, with a lateral extent limited to the equivalent of twice the tip's basal area. This cut-off defines the 'perturbation domain' (containing up to 30 inequivalent atoms). Its choice results from the fact that the energy levels and the electronic structures of the non-interacting semi-infinite metallic surfaces and nanotips are recovered at the boundaries of this domain.

Finally in this scheme, the band structure energy may be written as a sum of local energies over all the atoms constituting the system:

$$E_{bs} = \sum_i E_i^{bs} \qquad E_i^{bs} = \sum_\lambda \int^{\varepsilon_F} \varepsilon n_{i\lambda}(\varepsilon) \mathrm{d}\varepsilon - N_i \delta V_i$$

where ε_F is the Fermi level and $n_{i\lambda}(\varepsilon)$ the projected LDOS on the $|i\lambda\rangle$ states. The total LDOS is the sum of these partial LDOS over the 'd' orbitals. N_i is the 'd' band filling which depends only on the chemical nature of atom i and δV_i the electrostatic potential from the difference between the local energy level ε_i of the considered atom and the energy level of a bulk atom.

The repulsive energy E_r is chosen to be described by a pair potential of the Born–Mayer type:

$$E_r = \tfrac{1}{2} A \sum_{i,j \neq i} \mathrm{e}^{-pR_{ij}}.$$

The parameters A and p are fitted to obtain the bulk isotropic compressibility B_c and cohesive energy E_c. Then the calculated equilibrium lattice parameter a_0 is nearly equal to the experimental one. The values we have chosen for W are close to those of Gschneidner [21], i.e. $E_c = 8.52$ eV and $B_c = 2.02$ eV Å^{-3}/atom, the lattice parameter being $a_0 = 3.166$ Å.

2.2. Calculation of the local densities of states

The partial LDOS are calculated by the recursion method [22]: the Green's function on the considered $|i\lambda\rangle$ state is expanded as a continuous fraction with N exact levels, each level being associated with a pair of coefficients (a_n, b_n). Qualitatively, the calculation of the (a_n, b_n) coefficient consists in building up a new base of iterative $|n\}$ states obtained by applying the Hamiltonian on the starting $|i\lambda\rangle$ state and iteratively on all its successive nearest neighbours (with an orthonormalization procedure for the new $|n\}$ states). It is well known that in the absence of a gap in the band, the coefficients tend towards asymptotic values for $n \geqslant N$. When they are in their asymptotic regime, the fraction is terminated in the usual square root way. Here the asymptotic values (a_∞, b_∞) are obtained by the Beer–Pettifor method [23] which determines the exact value of the centre of the spectral support (a_∞) and the exact value of the spectral support's width $(4\sqrt{b_\infty})$ for the considered state.

For most of the cases we consider here, we have found that, for W tips and samples, the value $N = 8$ represents a satisfactory compromise between precision and computing time. Of course, we have verified that for $n \geqslant 8$ the (a_n, b_n) coefficients are in their asymptotic regime. As will be shown later, the LDOS obtained with $N > 8$ are not significantly different to those calculated with $N = 8$ (figure 3(c)).

2.3. The structure of the considered systems

The perfect tips are assumed to be the sharpest possible perfect pyramids (pyr) with a monatomic apex and are supported by a perfect semi-infinite bcc crystal (TSp). They are built from h perfect bcc (001) or (111) planes (see for example figure 1). In the later case, the tip's structure is the same as the one obtained experimentally by Vu Thien Binh and Garcia [5, 6]. We also considered truncated pyramids (tpyr). They are obtained from the perfect ones when suppressing the topmost atoms, so that they have multiatomic apexes with for example four or nine atoms for (001) planes and three or six for (111) planes. Finally and as a first step for such calculations, we do not consider in this study the relaxation or the reconstruction of the tip's support, nor the tip's relaxation. In order to clarify the importance of such an approximation, the role of the apex's relaxation on the LDOS has been studied (see below). Finally note that preliminary tight-binding molecular dynamics calculations have been performed [24]. They have shown, for example, that for Re the relaxation of the supported nanotips does not introduce significant changes of the electronic structure of such tips.

3. The electronic structure of transition metal nanotips

To clarify the role of the tip morphology and of the T/TSp interaction on the apex electronic structure, we have first calculated the electronic structure of supported W tips for h varying from one (an adsorbate) to six (subsection 3.1). We have also calculated it for isolated finite clusters and compared this to the supported tip case (subsection 3.2). From these calculations, we have also studied the stability of different supported tip morphologies (section 4).

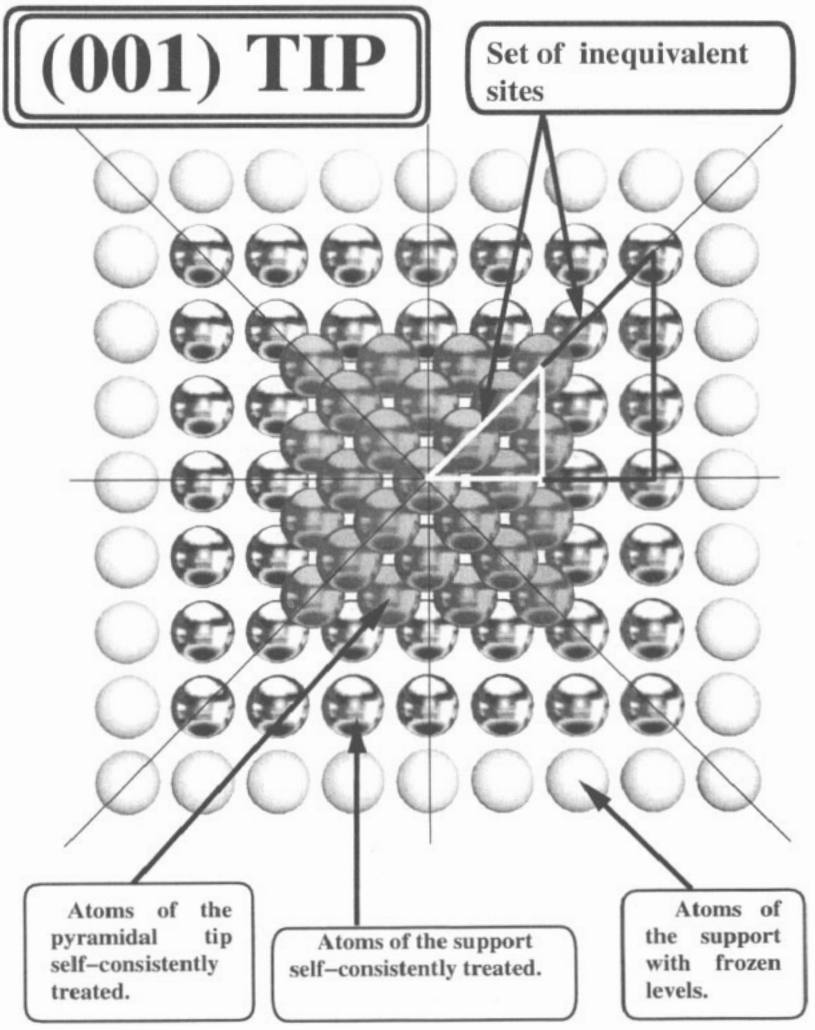

Figure 1. A schematic top view of the supported pyr(001) $h = 4$ tip. The perturbation domain is defined by the tip and tip support atoms which are labelled to be 'self-consistently' treated. It extends to the first three tip support (001) planes. Note that only a limited extent of the tip support surface plane is shown. Owing to symmetry properties, the inequivalent tip and tip support atoms are contained in the irreducible eighth (white and black triangles respectively).

3.1. The electronic structure of supported nanotips

The apex LDOS (aLDOS) width W_a is essentially determined by the number n_i of first- and second-nearest neighbours ($i = 1, 2$ respectively): $n_1 = 4$ and $n_2 = 1$ for pyr(001), $n_1 = 4$ and $n_2 = 3$ for pyr(111). W_a is independent of h and smaller than or equal to the width of the corresponding surface ($n_1, n_2 = 4, 5$ for (001); 4, 3 for (111)). Unlike the LDOS of the W(001) surface (figure 2(a)), no strong surface peak appears near the middle of the aLDOS.

For $h = 1$, the tip being reduced to a single adsorbate, the energy levels are strongly coupled with the surface W(001) peak so that the aLDOS is characterized by bonding and

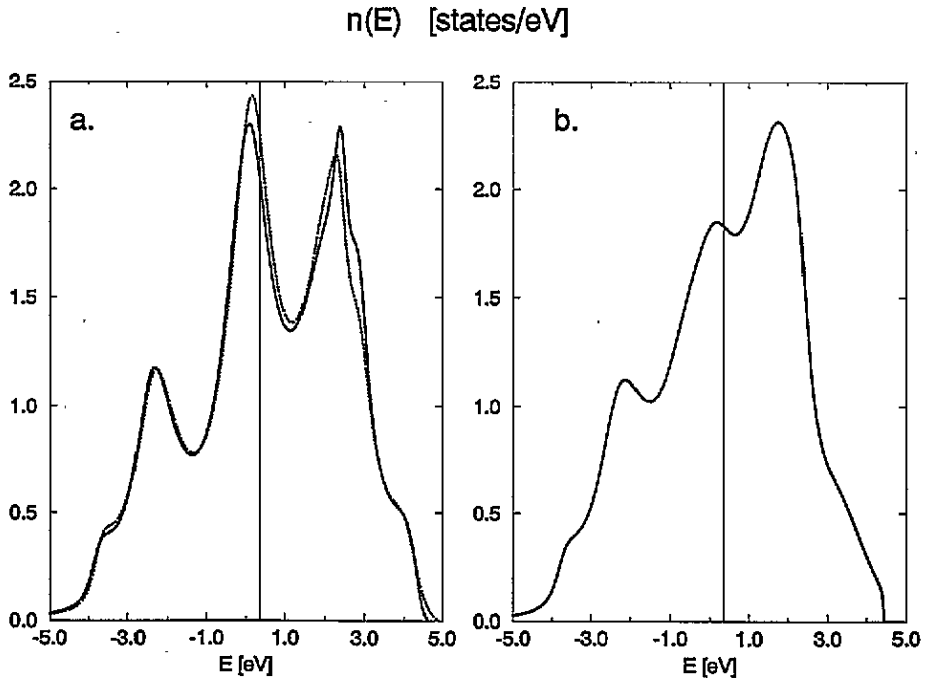

Figure 2. The LDOS of W(*hkl*) surfaces: (a) (*hkl*) = (001); (b) (*hkl*) = (111). The dotted line is the W(001) LDOS calculated with a hyperbolic cosine R dependence of $t(R)$. The energies are given in electron volts, the values of the densities of states are given in states per electron volt and the vertical line represents the Fermi level ε_F as in the following LDOS figures.

antibonding peaks (figure 3(a)). The aLDOS of pyr(001) for increasing h values is thus mostly characterized by such peaks which themselves become split into subpeaks. It is nearly independent of h for $h \geqslant 4$ (figure 3(b) and (c)).

The surface peak of the W(111) surface (figure 2(b)) being much less important than the W(001) one, the bonding–antibonding character of the pyr(111) aLDOS is less marked (figure 4(a)). Finally, this bonding–antibonding feature disappears for the LDOS of the atoms located on the top of a truncated pyramid with three apex atoms (figure 4(b)), these LDOS being similar to the corresponding surface LDOS.

In order to show the influence of the $t(R)$ analytical form, we study the W(001) and pyr(001) $h = 4$ apex LDOSs calculated with $t(R)$ decaying as a hyperbolic cosine as mentioned in section 2. The shape of these LDOS is not significantly modified (figures 2(a) and 3(b)). This illustrates that the assumption we use for the range for the hopping integrals is not essential, at least for the analytical forms we consider here.

As mentioned previously, it is important to estimate qualitatively the modifications of the LDOS upon tip relaxation. Therefore and as a first example, we have considered tips for which only the perpendicular distance d_a between the apex and the plane defined by its first-nearest neighbours can be changed. Let us first summarize the results for pyr(001) $h = 4$. When d_a increases, the aLDOS broadens and states are displaced towards the top and bottom of the band. Hence a hole appears in the middle of the aLDOS. In contrast, for increasing d_a values, the aLDOS narrows and states become closer to the centre of the band. The main modifications appear for the peaks just below and above the Fermi level ε_F. An analysis of these peaks according to the orbital symmetry shows that the peak above

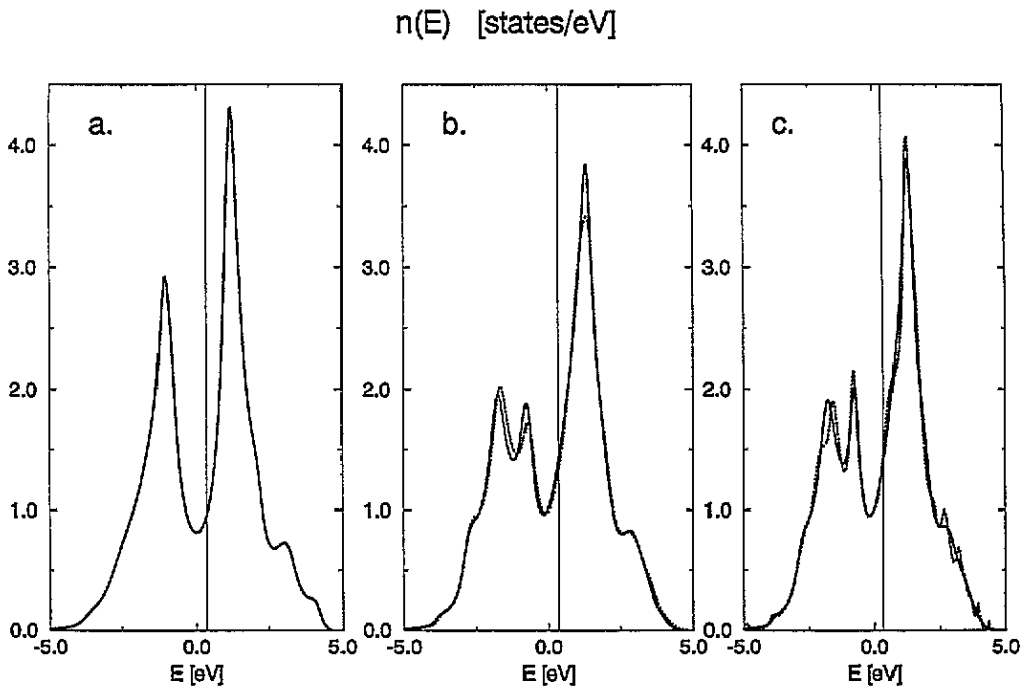

Figure 3. The aLDOS of a supported pyr(001) with (a) $h = 1$ (an adsorbate), (b) $h = 4$ (the dotted line is the corresponding aLDOS calculated with a hyperbolic cosine $t(R)$ form) and (c) $h = 6$. The dotted line is the corresponding aLDOS calculated with $N = 16$ recursion levels.

ε_F (A peak) originates mainly from the d_{z^2} and $d_{x^2-y^2}$ orbitals, whereas the peak below ε_F (B peak) originates from the d_{xy} orbital. While these peaks are displaced towards the band's centre, their amplitudes increase for increasing d_a values (figure 5(a)). However the B peak grows more rapidly than the A peak. In order to quantify the modifications of the aLDOS with respect to the apex relaxation distance d_a, we define the amplitude ratio AR (i.e. amplitude of A peak/amplitude of B peak) and observe a decrease of AR for increasing d_a values. For $d_a/d_{(001)} = 0.00, 1.10, 1.25$ we obtain AR= 2.04, 1.67, 1.31 respectively.

On the other hand, the modifications of the aLDOS versus d_a are less marked for a pyr(111) $h = 4$, as shown in figure 5(b). Note that the peaks' evolutions are not as obvious as for pyr(001). Nevertheless these calculations do not provide in a straightforward way a simple interpretation of the experimental results of Vu Thien Binh [8] concerning the field emission from nanotips. However note that the effects of the electric field must be included in the calculations in order to interpret their results.

3.2. The electronic structure of isolated clusters and T/TSp interaction

In order to understand the influence of the TSp on the tip's electronic structure, we study isolated clusters with the same morphology (i.e. symmetry and interatomic distances) as the supported nanotips.

These systems have a finite number of atoms, so the corresponding tight-binding Hamiltonian has a finite size. The discrete cluster energy levels are easily obtained by a diagonalization procedure. For comparison with the LDOS of supported tips, the discrete

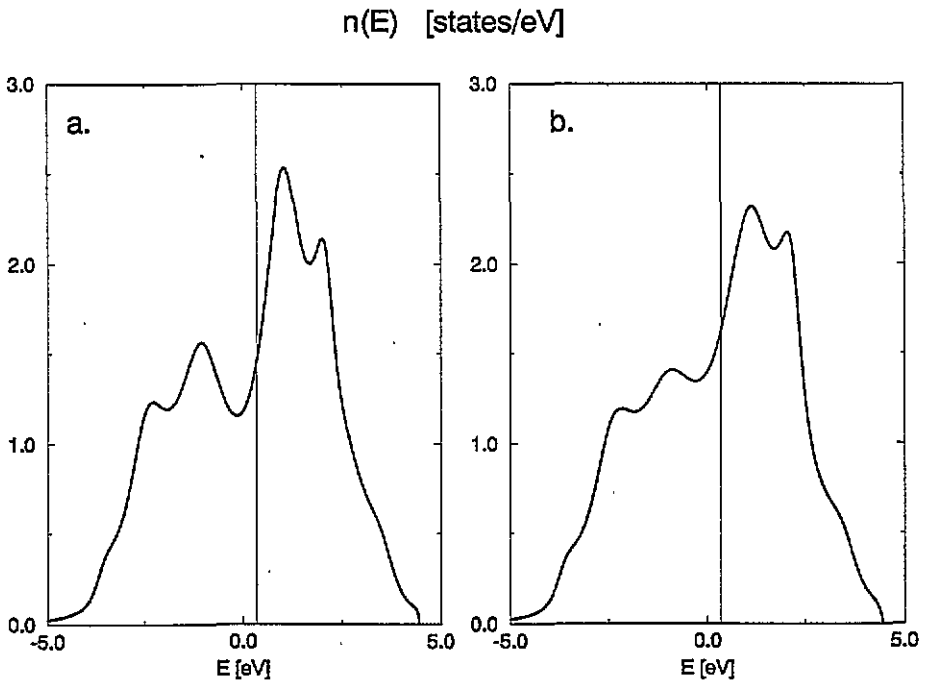

Figure 4. The aLDOS of a supported (a) pyr(111) $h = 4$, (b) tpyr(111) $h = 3$ with three apex atoms.

spectrum is convoluted with Lorentzians. Two self-consistent constraints have been used: (i) a self-consistent local neutrality, with an accuracy of 10^{-5} on each atom, to compare the cluster's LDOS with the supported tip ones, (ii) a self-consistent global neutrality ('Hartree–Fock' assumption) with an accuracy of 10^{-5} on the total number of electrons, to determine the magnitude of the charge transfers between the cluster's atoms and their roles in the apex electronic structure. For all these calculations, we have taken the same energy level reference, i.e. the energy level of a bulk atom.

Let us first discuss the electronic structure of the apex within the local neutrality assumption. The local environment (first- and second-nearest neighbours) of the apex is the same as for supported tips, but the aLDOS are quite different from those of the supported tips. For pyr(001) $h = 4$ (figure 6(a)), the shape of the aLDOS below the Fermi level differs from the one of the corresponding supported tip (figure 3(b)). However note that the peak just below ε_F originates from the d_{xy} orbital and the strong peak above ε_F is essentially due to the d_{z^2} and $d_{x^2-y^2}$ orbitals as for the supported tip. For pyr(111) $h = 4$ (figure 6(b)), the aLDOS exhibits strong differences from the corresponding supported tip aLDOS (figure 4(a)): the cluster aLDOS presents a more structured shape consisting of two pairs of peaks, one below and one above ε_F.

We conclude that the presence of the support (TSp) changes considerably the aLDOS, independently of the existence of the strong surface peak for the support. Consequently, *the use of finite-cluster aLDOS to describe the tip electronic structure in 'simple' STM models [12] is not appropriate, at least for the considered tip's structure.*

As a second step and in order to determine the modifications of the aLDOS due to charge transfers, we have also calculated the electronic structure of pyr(001) and pyr(111) $h = 4$ clusters within the 'Hartree–Fock' assumption. The charge transfers are obtained by

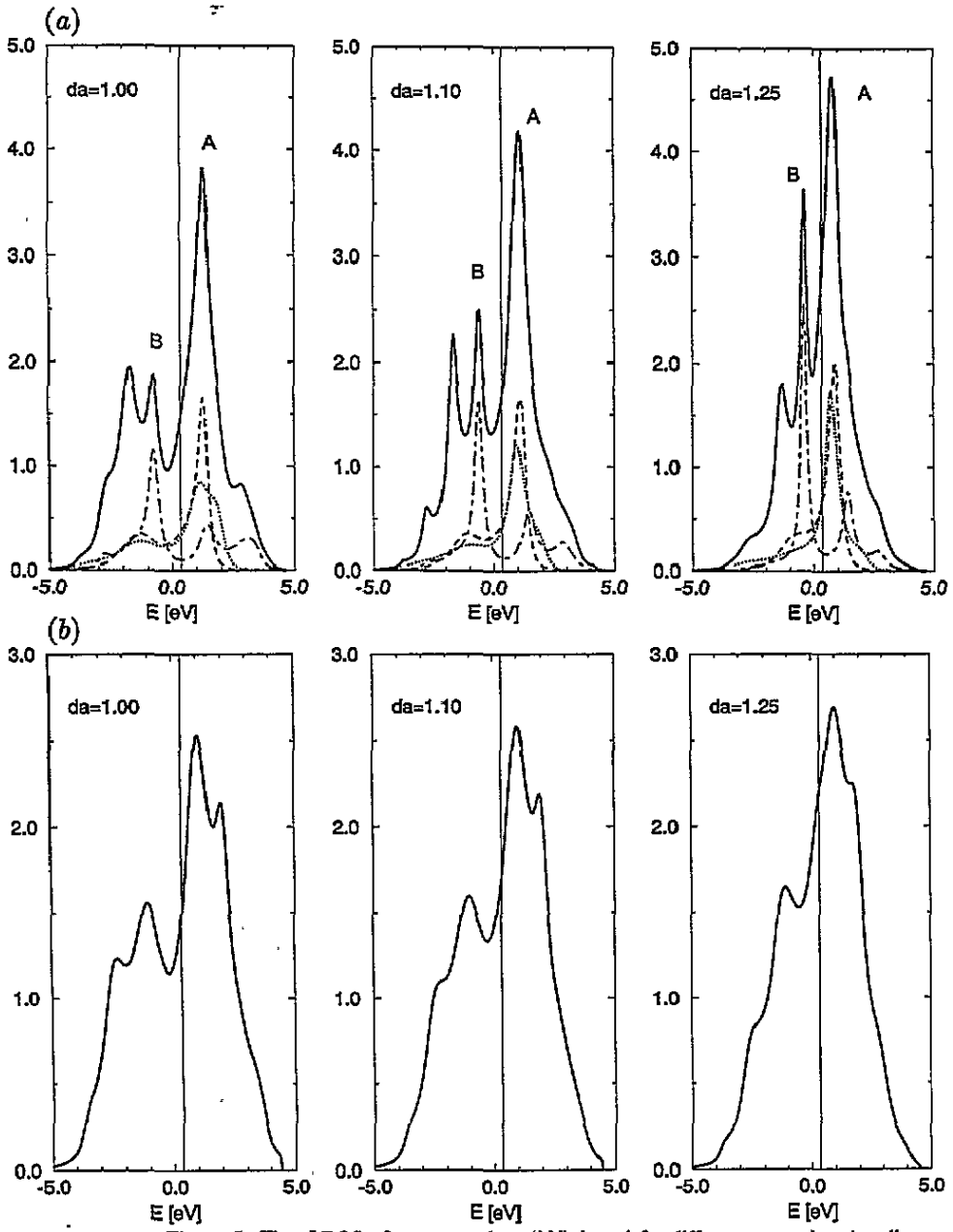

Figure 5. The aLDOS of a supported pyr(hkl) $h = 4$ for different apex relaxation distances d_a. d_a is defined as the perpendicular distance between the apex and the plane defined by its first-nearest neighbours. It is expressed in the interplanar $d_{(hkl)}$ unit. (*a*) $(hkl) = (001)$. The A peak comes mainly from the d_{z^2} and $d_{x^2-y^2}$ orbitals and the B peak from the d_{xy} orbital. The dotted line is the d_{z^2} orbital contribution to the aLDOS, the dashed line is for the $d_{x^2-y^2}$ orbital and the dot–dashed line for the d_{xy} orbital. (*b*) $(hkl) = (111)$.

introducing an effective Coulomb integral U [20]. The effect of U on each LDOS is to produce a shift of the centre of gravity of the considered band, this shift being proportional to $U\Delta N$, where ΔN is the difference between the actual band filling and that of the neutral

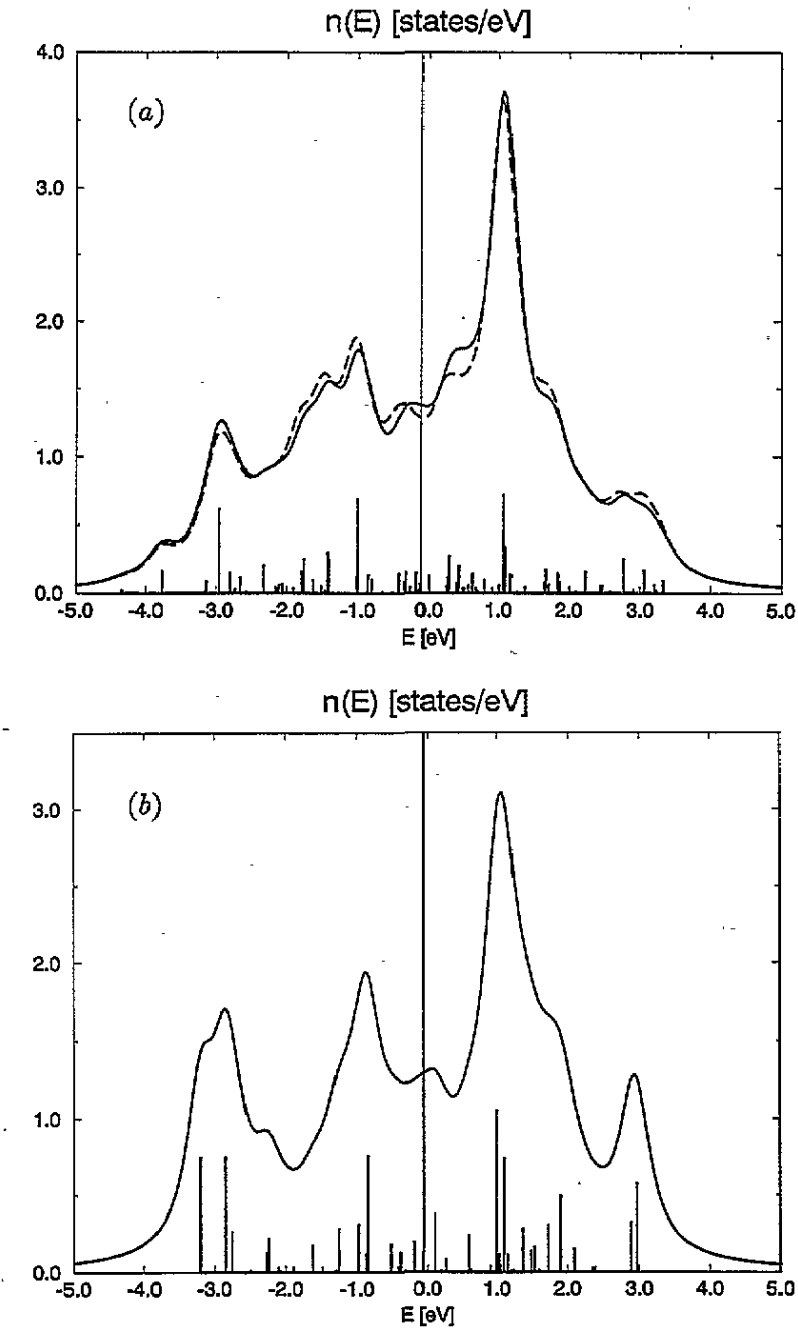

Figure 6. The aLDOS of isolated clusters. (*a*) pyr(001) $h = 4$; the dashed line is the corresponding aLDOS including charge transfers. Calculations are performed for $U/W = 0.05$. (*b*) pyr(111) $h = 4$. Each peak of the discrete spectrum is convoluted with a Lorentzian of 0.25 eV width.

atom. Calculations were performed for two extreme values of U, i.e. $U/W = 0.05$ and 0.18, as used in a previous work concerning the atomic structure of the W(001) surface [20].

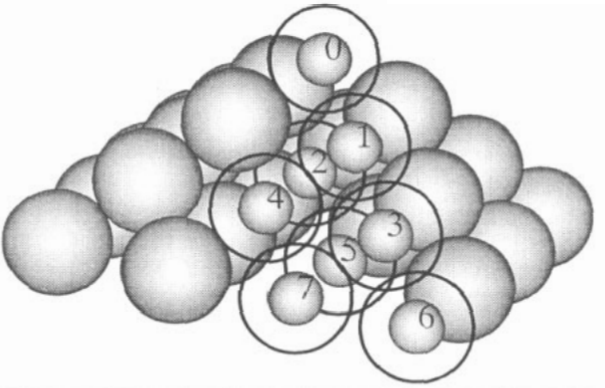

U/W	atom0	atom1	atom2	atom3	atom4	atom5	atom6	atom7
0.05	-0.075	-0.213	-0.148	0.011	-0.011	0.140	0.015	0.058
0.18	-0.047	-0.103	-0.084	0.010	-0.004	0.064	0.010	0.028

Figure 7. A schematic representation of the isolated pyr(001) $h = 4$ cluster. The inequivalent atoms of the cluster are represented by small spheres and are labelled from 0 to 7. Charge transfers for these atoms are calculated for both $U/W = 0.05$ and $U/W = 0.18$.

Figure 7 represents the pyr(001) $h = 4$ cluster and the charge transfers associated with each inequivalent atom. Qualitatively, charge is transferred from the apex to the pyramid's base. The largest loss of electrons appears on the apex and its nearest neighbours, especially on its four first-nearest neighbours (with $\Delta N = -0.213$) and its unique second-nearest neighbour (with $\Delta N = -0.148$). In fact, we observe a loss of electrons on the top three pyramid planes (apex included) ($\Delta N = -0.075$ for the apex and $\Delta N = -0.854$, -0.150 for the next two planes respectively) and a gain of nearly one electron ($\Delta N = +1.079$) on the pyramid's base. Despite the inclusion of charge transfers, the aLDOS is practically identical to the one calculated with the local neutrality assumption (figure 6(*a*)).

In conclusion, the charge transfers we obtain here do not strongly modify the LDOS. Furthermore, let us note that the large charge transfers observed especially on the tip's base are only valid for the case of isolated clusters. For supported tips and because of the screening properties of the metallic T and TSp, these charge transfers must be strongly reduced and affect only the tip's surfaces.

4. Nanotip stability and tip adsorption energy

We define the tip energy $E_T^{(h)}$ for various tip heights h and calculate it (within the local neutrality assumption and by the recursion method) for different tip morphologies. The tip energy is defined by

$$E_T^{(h)} = \sum_{i\in(T)}^{N_T}(E_i - E_{ref}) + \sum_{j\in(TSp)}(E_j - E_j^{(TSp)}) \tag{4.1}$$

where E_i is the contribution of the ith atom to the energy of the supported tip system, $E_j^{(TSp)}$ is the contribution of the jth atom to the energy of the isolated TSp, N_T is the number of

tip atoms and E_{ref} is the atomic energy reference. E_{ref} can be chosen either as the free atom's energy, i.e. $E_{ref} = 0$, or as the bulk cohesive energy, i.e. $E_c = -8.52$ eV/atom for W.

If E_{ref} is chosen to be the bulk cohesive energy, $E_T^{(h)}$ is the change of total surface energy between the supported tip system and the free semi-infinite crystal (TSp), i.e. the change in the total surface energy of a semi-infinite crystal when N_T bulk atoms are taken to create the tip on its surface. If we choose $E_{ref} = 0$, $E_T^{(h)}$ is the formation energy of the supported tip from its constituents (i.e. N_T isolated atoms). This last energy is the adsorption energy for the adsorbate (i.e. for pyr $h = 1$). We find $E_T^{(1)} = -8.63$ eV and -9.00 eV for the (001) and (111) planes respectively. These results are in good agreement with the previous theoretical work concerning the chemisorption of transition metal adatoms on transition metal surfaces [25]. Furthermore, the adsorption energy of W/W(111) is very close to the experimental value (8.8 eV) [26].

Note however that the adsorption energies $E_T^{(1)}$ are always smaller (larger in absolute value) than the cohesive energy E_c as in the previous work of Desjonquères *et al* [25]. This result is *a priori* surprising in the framework of a pair interaction model. However, as explained below this can be easily understood when studying the different contributions of the adsorbates and of the substrate on the adsorption energies.

The band energies of the adsorbates vary approximately as the square root of their coordination number Z [25] and their repulsive energies vary linearly with Z, so that the contribution of the adsorbates to $E_T^{(1)}$ is always larger (smaller in absolute value) than E_c, the adsorbates having a reduced coordination number as compared to a bulk atom. However, in the expression (4.1) the contribution of the substrate cannot be neglected. It represents approximately 40% of the adsorbate contribution to the adsorption energy and its value is such that the adsorption energy $E_T^{(1)}$ becomes smaller (greater in absolute value) than E_c. This result suggests that in the early stage of the homoepitaxial growth of W on W surfaces, the deposited atoms prefer to stay as isolated adsorbates on the surface rather than being condensed in small structures such as pyramids or flat islands. Furthermore, we have calculated the interaction energy between two adsorbates which are first-nearest neighbours on the W(001) surface. This energy is found to be repulsive (≈ 80 meV/atom) in agreement with an earlier work concerning the interaction of transition metal adatoms adsorbed on transition metal surfaces [27].

The results we obtain for the calculated values of $E_T^{(h)}$ for the different tip morphologies confirm this conclusion (see table 1). $E_T^{(h)}$ has been calculated with $E_{ref} = 0$, and $E_{T,at}^{(h)}$ is the tip formation energy per atom defined by $E_{T,at}^{(h)} = E_T^{(h)}/N_T$. We find that for all tip morphologies $E_T^{(h)} > N_T E_T^{(1)}$ for both pyr(001) and pyr(111).

The energy formation E_{flake} of a hexagonal flake containing 19 atoms (figure 8) deposited on the W(111) surface is slightly higher than the energy of the truncated tip tpyr(111) $h = 3$ made up of the same number of atoms. This means that once the tpyr is formed, it does not spread over the W(111) substrate like a flake. Furthermore, one can compare the formation energies for different systems containing the same number of atoms. Table 2 lists different configurations of N_T adsorbates ($N_T = 20$, 30 for (111), (001) planes respectively) according to increasing values of their energies. This suggests that starting from the N_T adsorbates, the tips can be formed step be step. The configuration of N_T isolated adsorbates is the lowest-energy configuration so energy barriers have to be overcome to form tips on the substrate for both the (001) and (111) planes. However, the energy values between the successive systems listed in table 2 are closer and closer, so one can guess that by simultaneous exchange of several atoms, the perfect pyr(001)

Table 1. Tip formation energies per atom $E_{T,at}^{(h)}$ calculated with $E_{ref} = 0$ for different tip morphologies.

Tip morphology	N_T	$E_{T,at}^{(h)}$ (eV/atom)
(001) planes		
pyr(001) $h = 1$[a]	1	−8.628
two pyr(001) $h = 1$[b]	2	−8.549
pyr(001) $h = 2$	5	−8.501
tpyr(001) $h = 2$[c]	25	−8.494
tpyr(001) $h = 3$[d]	29	−8.483
pyr(001) $h = 4$	30	−8.481
pyr(001) $h = 6$	91	−8.486
(111) planes		
pyr(111) $h = 1$[e]	1	−9.004
tpyr(111) $h = 3$[f]	19	−8.769
flake(111) $h = 1$	19	−8.742
pyr(111) $h = 4$	20	−8.762

[a] An adsorbate on a hollow site of the (001) surface (i.e. a site above the centre of a square of first surface nearest neighbours).
[b] Two adsorbates as in [a] which are the first surface nearest neighbours.
[c] Obtained from pyr(001) $h = 4$ suppressing the apex atom and its four first-nearest neighbours.
[d] Obtained from pyr(001) $h = 4$ suppressing the apex atom.
[e] An adsorbate on a hollow site of the (111) surface (i.e. a site above the centre of gravity of a triangle of first surface nearest neighbours).
[f] Obtained from pyr(111) $h = 4$ supressing the apex atom.

Table 2. Formation energies for different systems made up of N_T atoms. These energies are calculated with the $E_{T,at}^{(h)}$ values of table 1. The same notation is used as in table 1.

	Formation energy (eV/atom)
(111) planes, $N_T = 20$	
N_T adsorbates	−9.004
tpyr(111) $h = 3$ plus an adsorbate	−8.781
pyr(11) $h = 4$	−8.762
flake plus an adsorbate	−8.755
(001) planes, $N_T = 30$	
N_T adsorbates	−8.628
tpyr(001) $h = 2$ plus a pyr(001) $h = 2$	−8.495
tpyr(001) $h = 3$ plus an adsorbate	−8.488
pyr(001) $h = 4$	−8.481

or (111) $h = 4$ can be obtained without the need of large 'activation' energies. Tight-binding molecular dynamics calculations, taking into account the relaxation energies, are under progress to clarify this point.

We have also studied the T/TSp interaction energy by defining the tip adsorption energy E_{adsT}:

$$E_{adsT} = \sum_{i\in(T)}^{N_T} (E_i - E_i^{(T)}) + \sum_{j\in(TSp)} (E_j - E_j^{(TSp)}). \tag{4.2}$$

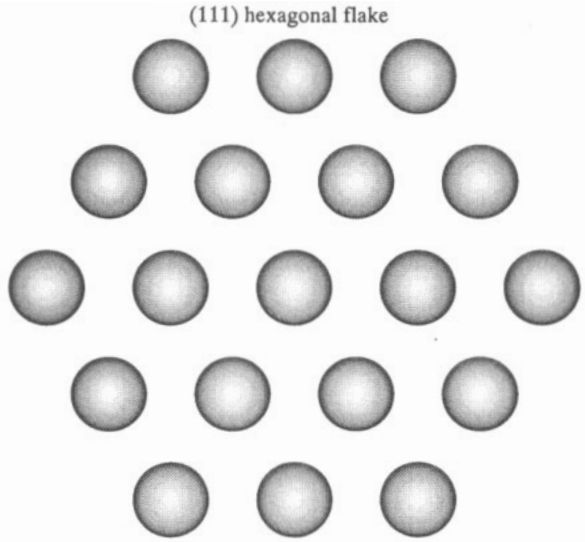

Figure 8. A schematic top view of the (111) hexagonal flake containing 19 atoms.

We use the same notations as in (4.1), the tip's atomic energy reference being $E_i^{(T)}$. We define $E_i^{(T)}$ as the contribution of the ith atom to the energy of the isolated cluster tip (containing N_T atoms) as calculated within the 'Hartree–Fock' assumption (with $U/W = 0.05$).

One finds $E_{adsT} = -68.392$ eV for pyr(001) $h = 4$, and $E_{adsT} = -71.445$ eV for pyr(111) $h = 4$. The tip's adsorption energy per atom $E_{adsT,at} = E_{adsT}/N_{T,b}$ (where $N_{T,b}$ represents the number of atoms of the tip's base, i.e. $N_{T,b} = 16$, 10 for the (001), (111) planes respectively) is $E_{adsT,at} = -4.274$, -7.144 eV/atom for pyr(001), (111) respectively.

Although the pyramid's base contains fewer atoms for the (111) than for the (001) pyramids, E_{adsT} is greater for the (111) than for the (001) planes. This is explained by the fact that there are more bonds between the atoms of the pyr(111) and its support than for the (001) case.

5. Conclusion

In this paper, we have investigated the electronic structure of W nanotips with different morphologies. We considered both supported nanotips and cluster tips. We used the tight-binding approximation to describe the band structure of the considered W nanotips and surfaces and we determined the local densities of states (LDOS) from the real space recursion method.

The study of the tip electronic structures has revealed the LDOS of supported tip apexes depends strongly on the tip's morphology. For perfect W supported tips pyr(hkl) $h = 1$–4, the apex LDOS are different from the ones of the corresponding W(hkl) surface (with (hkl) = (001) or (111)). These aLDOS become nearly independent of h for $h \geqslant 4$. In the case of truncated tips with multiatomic apexes, such as tpyr(111) $h = 3$, the aLDOS becomes similar to the surface LDOS. In order to determine the influence of the tip's support, the electronic structures of clusters having the same morphologies as the supported tips have been calculated. It is found that the electronic structures of such clusters are quite different from those of the supported tips. Hence it is not appropriate to use the electronic

structure of isolated clusters in order to calculate the tunnelling current between surfaces and tips modelled by such clusters. Moreover, the study of the tip stability has shown that perfect tips made up of N_T atoms are metastable systems as compared to N_T isolated adsorbates. However, it is possible to build up these tips step by step without needing large 'activation' energies. The general trends we obtain for the tip stability have to be examined in the scope of a tight-binding molecular dynamics scheme in order to confirm the previous conclusions. The study of the interaction of W supported tips with W perfect (or not) surfaces and a simple scheme to obtain atomic force images for such a system will be presented in a forthcoming paper [3].

References

[1] Binnig G, Rohrer H, Gerber Ch and Weibel E 1982 *Phys. Rev. Lett.* **49** 57
[2] Binnig G, Quate C F and Gerber Ch 1986 *Phys. Rev. Lett.* **56** 930
[3] Ness H and Gautier F 1995 *J. Phys.: Condens. Matter* 7 6641–61
[4] Fink H W 1988 *Phys. Scr.* **38** 260; 1990 *Scanning Tunneling Microscopy and Related Methods (NATO ASI Series E: Applied Sciences)* vol 184, ed R J Behm, N Garcia and H Rohrer (Dordrecht: Kluwer) p 399
[5] Binh V T 1988 *J. Microsc.* **152** 355; 1988 *Surf. Sci.* **202** L539
[6] Binh V T and Garcia N 1991 *J. Physique* I **1** 605
[7] Fink H W, Schmid H, Kreuzer H J and Wierzbicki A 1991 *Phys. Rev. Lett.* **67** 1543
[8] Vu Thien Binh, Purcell S T, Garcia N and Doglioni J 1992 *Phys. Rev. Lett.* **69** 2527
Garcia N, Vu Thien Binh and Purcell S T 1993 *Surf. Sci. Lett.* **293** L884
[9] Tersoff J and Hamann D R 1985 *Phys. Rev.* B **31** 805
[10] Bardeen J 1961 *Phys. Rev. Lett.* **6** 57
[11] Wintterlin J, Wiechens J, Brune H, Gritsch T, Höfer H and Behm R J 1989 *Phys. Rev. Lett.* **62** 59
Hallmark V M, Chiang S, Rabolt J F, Swalen J D and Wilson R J 1987 *Phys. Rev. Lett.* **59** 2879
[12] Ohnishi S and Tsukada M 1989 *Solid State Commun.* **71** 391
[13] Tsukada M and Shima N 1987 *J. Phys. Soc. Japan* **56** 2875
[14] Chen C J 1990 *Phys. Rev.* B **42** 8841
[15] Chen C J 1992 *Phys. Rev. Lett.* **69** 1656
[16] Friedel J 1969 *The Physics of Metals* ed J M Ziman (Cambridge: Cambridge University Press) p 494
[17] Desjonquères M C and Spanjaard D 1993 *Concepts in Surface Physics (Springer Series in Surface Science 30)* ed R Gomer (Berlin: Springer) p 218
[18] Slater J C and Koster G F 1954 *Phys. Rev.* **94** 1498
[19] Mattheiss L F 1965 *Phys. Rev.* **129** A 1893
[20] Treglia G, Desjonqueres M C and Spanjaard D 1983 *J. Phys. C: Solid State Phys.* **16** 2407
[21] Gschneidner K A 1964 *Solid State Physics* vol 16 (New York: Academic) p 275
[22] Haydock R 1980 *Solid State Physics* vol 35 (New York: Academic) p 215
[23] Beer N and Pettifor D G 1984 *The Electronic Structure of Complex Systems* ed P Phariseau and W M Temmerman (Plenum: New York) p 769
[24] Pizzagalli L, Bouette S, Stoeffler D and Gautier F to be published
[25] Desjonquères M C and Spanjaard D 1982 *J. Phys. C: Solid State Phys.* **15** 4007
[26] Menand A and Gallot J 1974 *Rev. Physique Appl.* 9 323
[27] Burke N R 1976 *Surf. Sci.* **58** 349